



## An electrochemically roughened Cu current collector for Si-based electrode in Li-ion batteries



David Reyter<sup>a</sup>, Steeve Rousselot<sup>a</sup>, Driss Mazouzi<sup>b,c</sup>, Magali Gauthier<sup>a,b,c</sup>, Philippe Moreau<sup>b,c</sup>, Bernard Lestriez<sup>b,c</sup>, Dominique Guyomard<sup>b,c</sup>, Lionel Roué<sup>a,\*</sup>

<sup>a</sup> INRS – Énergie, Matériaux et Télécommunications, 1650 boulevard Lionel Boulet, Varennes, Québec J3X 1S2, Canada

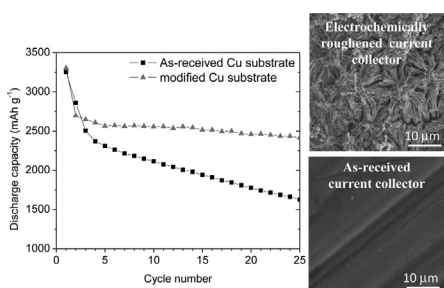
<sup>b</sup> Institut des Matériaux Jean Rouxel (IMN), Université de Nantes, CNRS, 2 rue de la Houssinière, BP 32229, 44322 Nantes Cedex 03, France

<sup>c</sup> Réseau sur le Stockage Electrochimique de l'Energie (RS2E), FR CNRS 3459, France

### HIGHLIGHTS

- Si-based anodes with electrochemically roughened current collector were studied.
- The Cu nanowires on the current collector enhance the adhesion of the Si coating.
- This limits the electrical disconnection of the Si particles with cycling.
- This results in an great improvement of the electrode cycle life.

### GRAPHICAL ABSTRACT



### ARTICLE INFO

#### Article history:

Received 7 February 2013

Received in revised form

14 March 2013

Accepted 20 March 2013

Available online 2 April 2013

#### Keywords:

Lithium-ion battery

Silicon-based anode

Current collector

Cycle performance

### ABSTRACT

An electrochemically roughened copper foil was evaluated as a current collector for micrometric Si powder (ball-milled) based electrodes prepared by the conventional slurry-coating method. The formation of a bunch of copper nanowires on the current collector provides a rough surface, which enhances the adhesion of the Si composite electrode as confirmed from scratch tests. This produces a major decrease of the irreversible capacity associated with the electrical disconnection of the Si particles with cycling, which results in a great improvement of the electrode cycle life. With such a roughened Cu current collector, the micrometric Si-based electrode is able to maintain a discharge capacity of  $1200 \text{ mAh g}^{-1}$  for at least 1000 cycles.

© 2013 Elsevier B.V. All rights reserved.

### 1. Introduction

A significant increase in the energy density of Li-ion batteries is required to fulfil the future demands for electronic devices, hybrid/electric vehicles and clean energy storage. In this context, silicon-based anode materials have attracted attention due to their

extremely high theoretical gravimetric and volumetric capacities ( $3572 \text{ mAh g}^{-1}$  and  $8322 \text{ mAh cm}^{-3}$  for  $\text{Li}_{15}\text{Si}_4$ ) compared to those of commercialized graphite-based anodes ( $372 \text{ mAh g}^{-1}$  and  $818 \text{ mAh cm}^{-3}$  for  $\text{LiC}_6$ ). Furthermore, silicon is an ideal choice element in terms of worldwide abundance and cost. However, this material suffers from poor cyclability because of its large volumetric change (up to 300%) during lithiation/delithiation processes leading to the so-called pulverization of Si particles and disintegration of the composite electrode architecture, resulting in the loss of electrical contact [1,2]. Another limitation is the formation of an

\* Corresponding author. Tel.: +1 514 228 6985; fax: +1 450 929 8102.

E-mail address: roue@emt.inrs.ca (L. Roué).

unstable solid electrolyte interphase (SEI) resulting in severe electrolyte degradation at the surface of the Si material, which induces a low coulombic efficiency and an increase of the electrode polarization resistance with cycling [3–5]. As recently reviewed in Refs. [6–8], several strategies have been developed to solve these problems, including: (i) the dispersion of Si in a composite matrix to buffer its large volume change; (ii) the use of nanosized Si (nanoparticles, nanowires, nanotubes, and thin films) that is better able to accommodate large strain without cracking; (iii) the use of capacity constraint limitations to minimize volume changes; (iv) the use of binders (e.g. carboxymethyl cellulose) favouring a resilient bonding between the Si and the conductive carbon black particles; and (v) the use of electrolyte additives (e.g. fluoroethylene carbonate) favouring the formation of a denser and more stable SEI.

Another relevant approach that could complement the previous strategies is to optimize the current collector architecture in order to minimize the loss of electrical contact between the active Si material and the current collector with cycling. For that purpose, the most common method is to produce porous or rough substrates (Ni, Cu) by sand-papering [9–11], chemical [12–14] or electrochemical [15] etching and electrodeposition [14,16–19]. Such substrate treatments allow obtaining Si-based thin films with better adhesion, lower electrical contact resistance and longer cycle life than those deposited on a smooth Cu foil. It was shown that the use of three-dimensional substrates (such as Cu foam [20], Cu macroporous sheet [21], carbon fibres [22] and Ni nanowires [23]) could also improve the cycle life of Si films thanks to their good adhesion to the high surface area current collector. More recently, a method consisting of the deposition of Si thin films on a soft (elastomeric) substrate to release the lithiation-induced stress has also demonstrated its efficiency to increase the electrode cycle life [24]. However, all these studies involve Si thin film electrodes having a low ratio of active material to substrate mass and requiring costly deposition methods (such as sputtering, pulsed laser deposition, vacuum deposition or e-beam deposition), which limit their practical application in Li-ion batteries.

To the best of our knowledge, only three papers [25–27] have paid attention to the effect of the current collector morphology on the cycle performance of Si-based electrodes prepared by the conventional slurry-coating method. Kim et al. [25] have shown that the cycle life of a mixed Si–C composite electrode is improved by using a nodule-type Cu current collector produced by an electroplating process. Such an electrode displayed a specific capacity of  $\sim 750 \text{ mAh g}^{-1}$  after 40 cycles versus  $\sim 300 \text{ mAh g}^{-1}$  for the electrode prepared with a flat Cu current collector. After cycling, only micro-cracks were observed and the structural integrity of the electrode was maintained with the nodule-type substrate, suggesting that the latter helps to maintain a good electrical contact between the electrode layer and the current collector. Jiang et al. [26] evaluated anodes prepared by casting slurries of milled Si powder onto a 3D Cu cellular architecture fabricated by multistep electrodeposition, resulting in improved cycling performance with the completion of 63 cycles at a limited capacity of  $800 \text{ mAh g}^{-1}$ , compared to 39 cycles by using a flat copper foil substrate. The improved cycle life was mainly attributed to the stress-alleviated environment coming from the 3D substrate architecture. More recently, Ni foam was evaluated as current collector for nanosized Si-based electrodes [27]. A remaining discharge capacity of  $350 \text{ mAh g}^{-1}$  was obtained after 95 cycles versus  $0 \text{ mAh g}^{-1}$  for an electrode prepared with a flat Cu foil current collector. These various studies confirm the relevance of using current collectors with unconventional architecture for improving the cycle life of Si-based anodes. However, major research efforts have to be extended to reach the cycling stability required for practical application in Li-ion batteries.

In this study, we report the preparation and characterization of an electrochemically roughened copper substrate. This current collector is described as a copper nanowire architecture formed on the original smooth copper foil. Its influence on the cycle performance of micrometric Si powder (ball-milled) based electrodes prepared by the conventional slurry-coating method is investigated.

## 2. Experimental

### 2.1. Cu substrate preparation and characterization

We evaluated different methods for the surface modification of the copper substrate, including chemical etching in various solutions, Cu electrodeposition and electrochemical treatments using different protocols. The best results (in term of cycle life improvement) were obtained using the following procedure. Experiments were performed in 1 M NaOH using a three-electrode one-compartment cell containing a rectangular copper foil (99.5%, 25  $\mu\text{m}$  thick, Alfa Aesar) as working electrode, a nickel grid (99.5%, 20 mesh, Alfa Aesar) as counter electrode of the same geometric surface area ( $150 \text{ cm}^2$ ) and an Hg/HgO reference electrode. The copper electrode was cycled 3000 times at  $10 \text{ V s}^{-1}$  between  $-1.6$  and  $1 \text{ V}$  vs. Hg/HgO. After the electrochemical treatment, the sample was rinsed with deionized water, dried and annealed at  $300^\circ\text{C}$  for 3 h under Ar/5%  $\text{H}_2$  (1 atm). The morphological characterization of the Cu substrate was performed using a Jeol JSM-6300F scanning electron microscope (SEM). X-ray diffraction (XRD) measurements were carried out at a grazing angle of  $2^\circ$  using a Bruker AXSD8 Siemens X-ray diffractometer with  $\text{Cu K}\alpha$  radiation ( $1.54 \text{ \AA}$ ).

### 2.2. Si powder synthesis and characterization

Silicon powder (99.999%, 20 mesh, Cerac) was milled under argon for 20 h using a SPEX 8000 mixer. The ball-to-powder mass ratio was 5:1. The milled Si powder consists of micrometric agglomerates (median size  $\sim 6 \mu\text{m}$ ), made of submicrometric cold-welded particles with crystallite size of  $\sim 10 \text{ nm}$ . More details on the structural, morphological and surface chemical characteristics of the milled Si powder are presented elsewhere [28,29].

### 2.3. Composite electrode preparation and characterization

Milled Si powder was used as the active material, Super P carbon black (noted CB,  $60 \text{ m}^2 \text{ g}^{-1}$ , TIMCAL) as the conductive agent, and carboxymethyl cellulose (noted CMC, DS = 0.7, Mw = 90,000, Aldrich) as the binder. A mixture of 200 mg of active material + CB + CMC in a weight ratio of 80:12:8 was introduced into a silicon nitride vial containing three silicon nitride balls (9.5 mm diameter). Then, 0.5 mL of 0.173 M citric acid + 0.074 M KOH buffer solution at pH 3 was added and the mixture was milled at 500 rpm for 1 h using a Fritsch Pulverisette 7 mixer. As shown previously [30], the buffering at pH 3 promotes covalent bonding (esterification) between  $-\text{OH}$  groups present on the surface of Si particles and  $-\text{COOH}$  groups of CMC, which significantly improves the electrode cycle life. The electrode was made by casting with a doctor blade the slurry onto either the modified or the as-received copper current collector. Finally, it was dried for 12 h at room temperature and then 2 h at  $100^\circ\text{C}$  under vacuum. Citric acid (16.62 mg) and KOH (2.08 mg) from the buffer solution did not evaporate during the drying process and thus contribute to the mass of electrodes, leading to a Si/C/CMC/(citric acid + KOH) wt.% compositions of 73.1/11.0/7.3/8.6. The adhesion strength of the deposit on the modified and unmodified Cu substrate was evaluated by scratch testing done

at room temperature with a balanced beam scrape adhesion and mar tester (BYK-Gardner) according to the ASTM D2197 standard method. In addition, a piece of Scotch brand tape was pressed onto the electrode and then quickly removed. The boundary region near the peeled film was observed by cross-sectional SEM analysis.

#### 2.4. Electrochemical measurements

Two-electrode Swagelok cells were used for the cycling tests. The cells were assembled in a glove box under argon atmosphere and consisted of a  $1\text{ cm}^2$  disc of composite anode containing typically 0.7 mg of active Si material, a GF/D borosilicate glassfiber sheet from Whatman as separator and a  $1\text{ cm}^2$  Li metal disc as the negative and reference electrode. Unless otherwise indicated, the electrolyte was 1 M LiPF<sub>6</sub> in 1:1 ethylene carbonate (EC)/dimethyl carbonate (DMC) from Novolyte. Unless otherwise indicated, cycling tests were carried out at 20 °C on an Arbin BT2000 system in the voltage range 0.005–1 V (vs. Li+/Li) at a current density of 600 mA g<sup>-1</sup> of Si both in discharge (lithiation) and charge (delithiation) with no capacity limitation. All electrode capacities are given per gram of Si.

### 3. Results and discussions

#### 3.1. Characterization of the current collector and the adhesion strength of the Si-based coating

Prior to coating with active material, the surface of the copper substrate was examined by SEM (Fig. 1) and XRD (Fig. 2) in as-received state, after electrochemical modification and after a subsequent reductive annealing treatment. As previously shown by Reyter et al. [31], Cu(OH)<sub>2</sub> needles grow on the copper substrate during fast potential cycling (10 V s<sup>-1</sup>) in 1 M NaOH between the hydrogen evolution reaction and the oxygen evolution reaction. The electrochemical formation of Cu(OH)<sub>2</sub> on the Cu substrate is confirmed from XRD analysis (Fig. 2b). After 3000 cycles, the mean diameter and length of these needles are approximately 0.2 and 5 μm, respectively (Fig. 1b). After subsequent annealing under H<sub>2</sub> atmosphere, the Cu(OH)<sub>2</sub> needles are converted to a bunch of metallic copper nanowires making a rough and nanostructured surface (Fig. 1c). These nanowires have a diameter constrained to tens of nanometers and a length of approximately 5 μm. The complete conversion of Cu(OH)<sub>2</sub> to metallic copper is confirmed by XRD analyses performed after the reduction treatment (Fig. 2c).

Fig. 3 shows cross-sectional SEM images of the Si-based film deposited on as-received (a) and electrochemically modified (b) copper substrates after a scotch tape peel test. The SEM images

show both coated and peeled zones. The detachment of the film from the Cu substrate along the track of the tape is more pronounced on the as-received substrate. Indeed, by examining the peeled region, it clearly appears that no Si-graphite material remained on the flat copper foil (Fig. 3a) while a thin deposited layer is still present on the modified substrate (Fig. 3b). This reveals the better adhesion of the Si-based coating on the modified current collector. This is also supported by scratch tests, indicating a mar-resistance (determined as the minimum load in grams required to cut through the film to the substrate) of 40 and 110 g for the electrode prepared with the as-received and modified Cu substrate, respectively.

#### 3.2. Electrochemical behaviour

A typical evolution of the discharge–charge curves with cycling (25 cycles) of the Si-based electrodes prepared with as-received and modified Cu substrates is shown in Fig. 4a and b, respectively. For both electrodes, a decrease of the discharge and charge capacities with cycling is observed. However, this decay is significantly lower for the electrode prepared with the modified Cu substrate. This is highlighted in Fig. 5, which shows the evolution of the discharge capacity with cycling for both electrodes. As a result, the latter displays a capacity of 1630 mAh g<sup>-1</sup> after 25 cycles versus 2410 mAh g<sup>-1</sup> for the electrode with the roughened current collector.

In addition, by comparing their respective discharge–charge curves in Fig. 4a and b, it appears that the progressive shift of the discharge and charge potentials with cycling, reflecting an increase of the electrode polarisation resistance, is lower with the modified substrate based electrode. This is confirmed in Fig. 6, which shows the evolution with cycling (from the 2nd to the 25th cycle) of the polarization resistance ( $R_p$ ) of the electrodes.  $R_p$  was determined from the voltage difference at half charge and half discharge capacities divided by the current. The  $R_p$  of the unmodified-substrate electrode rapidly increases from 610 to 690 Ω between the 2nd and the 10th cycles. During the following cycles, its increase is much slower and  $R_p$  reaches 700 Ω at the 25th cycle. For the modified substrate based electrode, the initial  $R_p$  value is significantly lower (525 Ω) and no major rise of  $R_p$  is observed during the first 10 cycles in contrast to what was observed with the unmodified-substrate electrode. At the 25th cycle,  $R_p$  reaches 570 Ω.

The increase of  $R_p$  with cycling may have two main origins: (i) the formation of a blocking SEI layer on Si particles that grows with cycling, which limits Li salt diffusion into the pores of the composite electrode and thus increases its polarization resistance [4]; or (ii) the huge volume variation of the Si particles during the

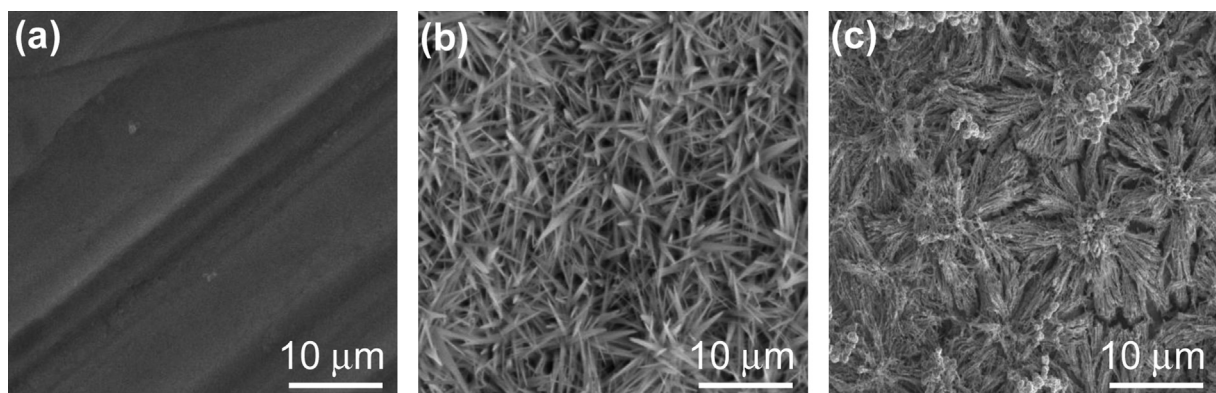


**Fig. 1.** SEM micrographs of the (a) as-received Cu substrate, (b) after electrochemical treatment and (c) subsequent reductive annealing treatment.

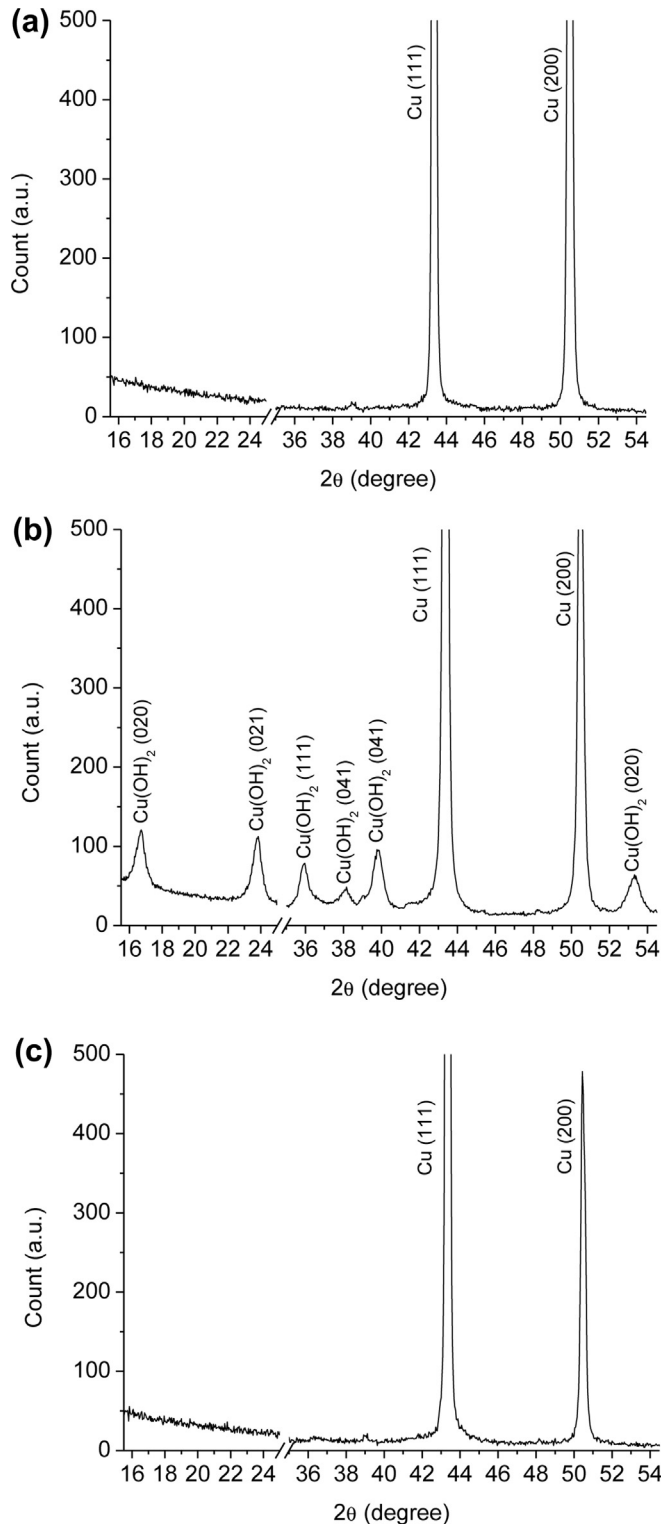


**Fig. 2.** XRD patterns of the (a) as-received Cu substrate, (b) after electrochemical treatment and (c) subsequent reductive annealing treatment.

lithiation/delithiation processes leading to cracking of the Si particles and subsequent disintegration of the composite electrode architecture, resulting at worst in a loss of electrical contact or at least in an increase of the contact resistances at the particle/current collector and particle/carbon interfaces [2]. It can be assumed that the modification of the Cu current collector has no effect on the SEI

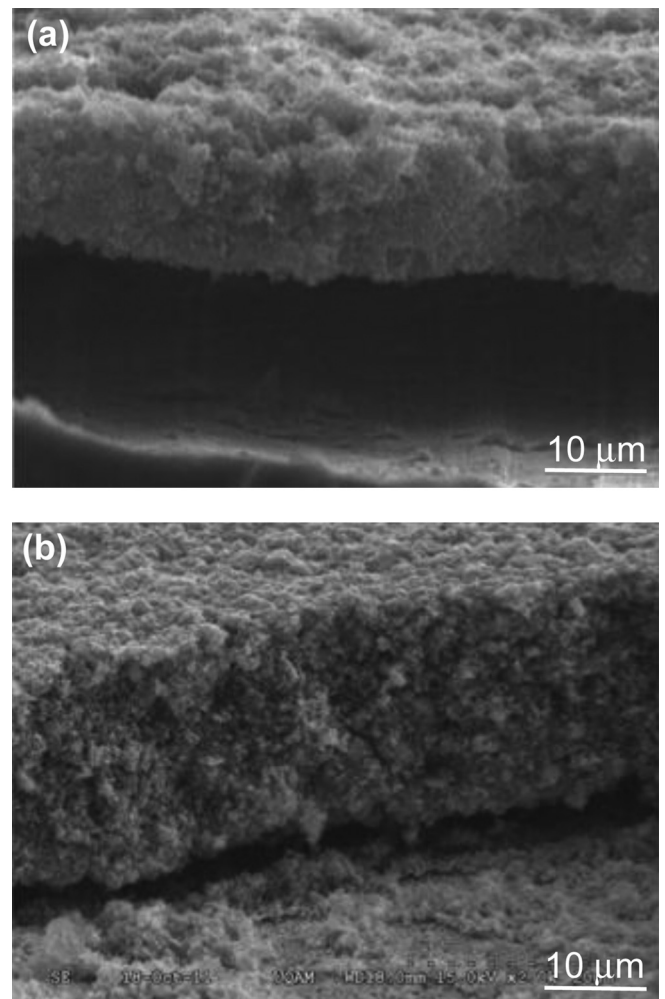


**Fig. 3.** Cross-sectional SEM images of the Si-based film deposited on (a) as-received and (b) modified copper substrates after a scotch tape peel test.

formation kinetics and Si particle cracking intensity. Thus, the lower and more stable  $R_p$  (Fig. 6) as well as the better capacity retention (Fig. 5) observed with the modified substrate based electrode must be essentially due to the higher adhesion strength of the Si-based film on the roughened Cu collector as shown previously from scratch tests. This better adhesion helps to maintain a good electrical contact between the current collector and the Si composite film despite the severe volume variation and cracking of the silicon particles.

In order to confirm that the electrical disconnection of the Si particles is lower with the modified Cu substrate, we attempt to determine on both electrodes the irreversible capacity related to this disconnection issue. To this end, as a first approximation, it is assumed that the irreversibility due to disconnection occurs mostly during the charge, *i.e.* when the particles deflate upon dealloying [2]. The irreversible capacity associated with the electrical disconnection of the Si particles ( $IC_{DISCONN.}$ ) is thus defined as:

$$IC_{DISCONN.} = C_n - C_{n+1} \quad (1)$$

where  $C_n$  is the charge capacity at cycle  $n$  and  $C_{n+1}$  is the charge capacity at cycle  $n + 1$ .

On the other hand, the SEI is almost exclusively generated during the discharge [32] and thus the capacity corresponding to

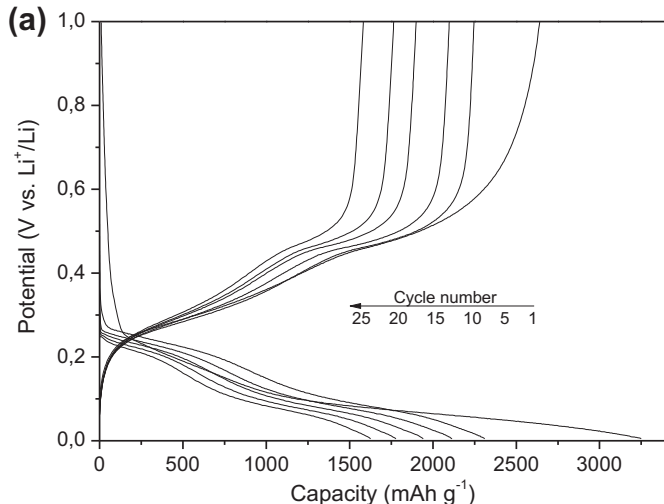


**Fig. 4.** Galvanostatic discharge–charge curves (cycles 1, 5, 10, 15, 20, 25) of the Si-based electrodes prepared with (a) as-received and (b) modified Cu substrates.

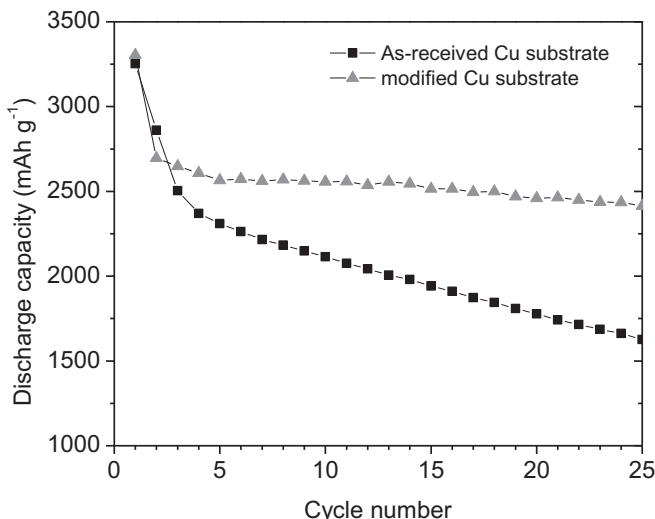


**Fig. 5.** Evolution with cycling of the discharge capacity of the Si-based electrodes prepared with as-received and modified Cu substrates.

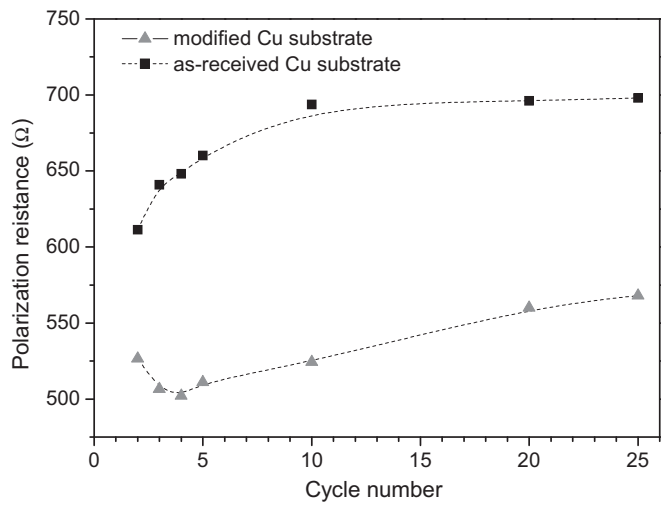


**Fig. 6.** Evolution with cycling of the polarization resistance of the Si-based electrodes prepared with as-received and modified Cu substrates.

the formation of the SEI is considered to be the difference between the discharge capacity at cycle  $n + 1$  and the charge capacity of the previous cycle  $n$ . Consequently, the irreversible capacity related to the SEI ( $IC_{SEI}$ ) can be determined as:

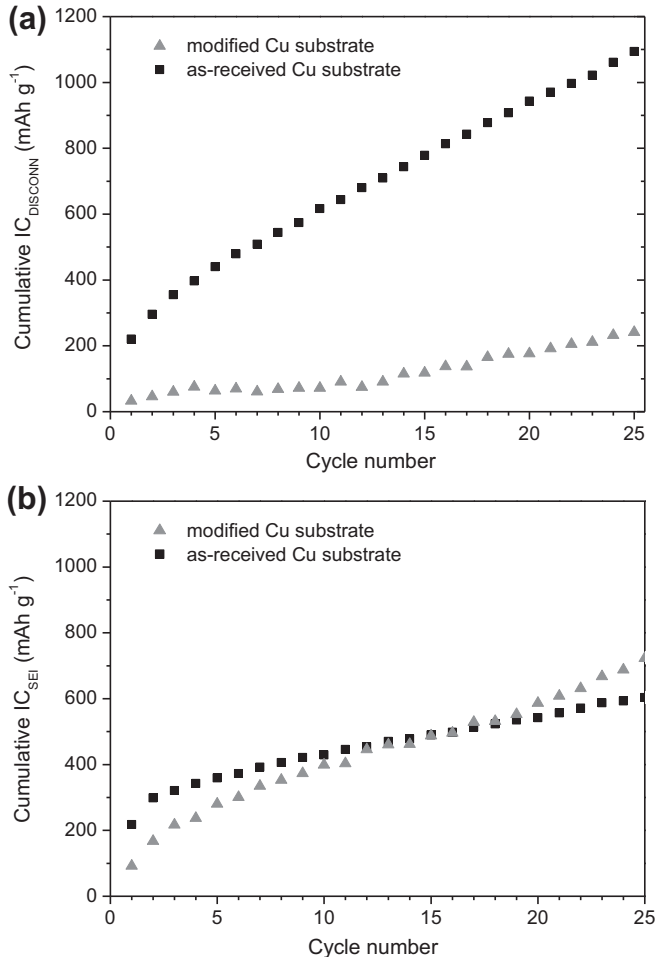


**Fig. 7.** Evolution with cycling of the cumulated irreversible capacity related to the electrical disconnection of the Si particles ( $IC_{DISCONN.}$ ) (a) and of the cumulated irreversible capacity related to the SEI ( $IC_{SEI}$ ) (b) for the Si-based electrodes prepared with as-received and modified Cu substrates.

$$IC_{SEI} = D_{n+1} - C_n \quad (2)$$

where  $D_{n+1}$  is the discharge capacity at cycle  $n + 1$  and  $C_n$  is the charge capacity at cycle  $n$ .

The evolutions with cycling of cumulated  $IC_{DISCONN}$ , and  $IC_{SEI}$  for both electrodes are shown in Fig. 7a and b, respectively. A great decrease (by a factor of  $\sim 5$  after 25 cycles) of the irreversibility associated with the disconnection of particles is observed with the modified substrate based electrode (Fig. 7a), confirming that the electrochemical roughening of the substrate significantly improves the mechanical stability of the Si coating on the current collector. In addition, one can note that  $IC_{DISCONN}$  increases rapidly during the first 3 cycles with the as-received substrate based electrode. This agrees with the fact that the Si particle cracking and electrode disintegration phenomena are at their maximum intensity during the first 3 cycles as recently shown from in-situ acoustic emission measurements [33]. Regarding the evolution of the irreversibility related to the SEI formation (Fig. 7b), no major difference can be noted between the electrodes, confirming that the modification of the Cu current collector has no effect on the SEI formation.

Previous works have shown that the addition of FEC and VC in the electrolyte in combination with the grafting of the CMC binder induces the formation of a more stable SEI on Si electrodes, resulting in a better stability of the capacity upon cycling [5]. Thus,

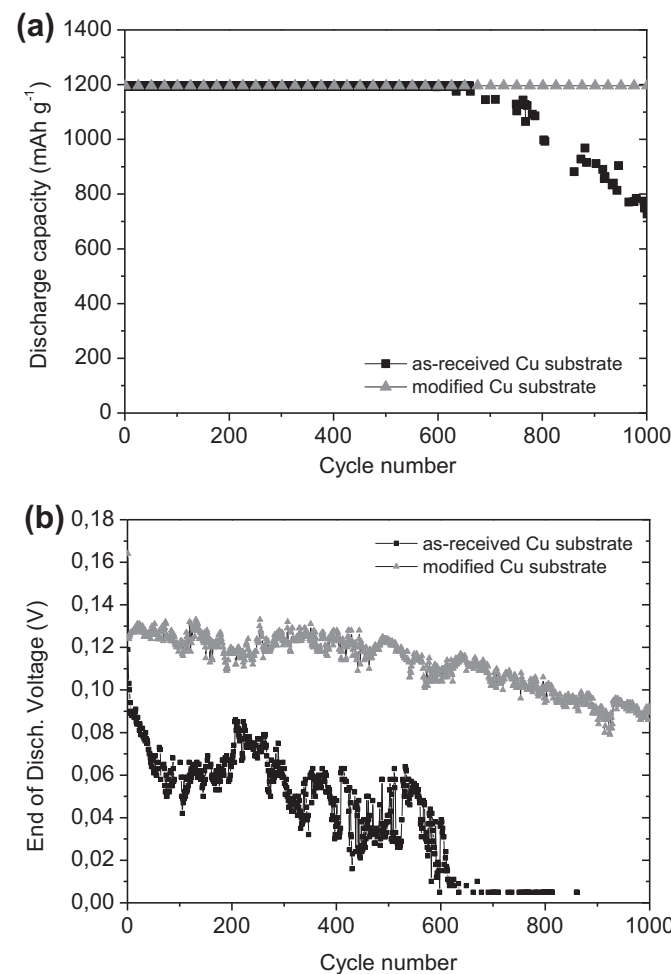


**Fig. 8.** Evolution with cycling of the (a) discharge capacity and (b) end-of-discharge voltage of Si-based electrodes prepared with as-received and modified Cu substrates for a discharge capacity limited to  $1200 \text{ mAh g}^{-1}$  in electrolyte with FEC + VC additives. The electrode Si loading is  $0.8 \text{ mg cm}^{-2}$ . The C-rate is  $1\text{Li/Si in } 2 \text{ h}$ .

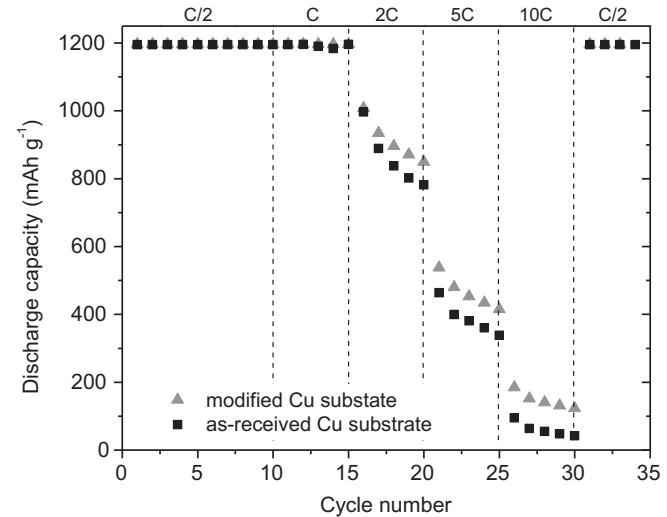


**Fig. 9.** Rate performance of Si-based electrodes prepared with as-received and modified Cu substrates for a discharge capacity limited to  $1200 \text{ mAh g}^{-1}$  in electrolyte with FEC + VC additives. The electrode Si loading is  $0.7 \text{ mg cm}^{-2}$ . A rate of 1C corresponds to  $1\text{Li/Si in } 1 \text{ h}$  (i.e.,  $960 \text{ mA g}^{-1}$ ) in discharge and charge.

a prolonged cycle life test was undertaken in 1:1 EC/DEC with 10 wt. % fluoroethylene carbonate (FEC) and 2 wt. % vinylidene carbonate (VC) on the Si-based electrode prepared with modified and unmodified Cu substrates. With a discharge capacity limited at  $1200 \text{ mAh g}^{-1}$  of Si for 1000 cycles, the electrode prepared with the modified Cu substrate exhibits an impressive stability whereas a decay in the discharge capacity is observed from about 600 cycles with the unmodified Cu substrate based electrode (Fig. 8a). Besides, as shown in Fig. 8b, the end-of-discharge voltage is higher and more stable for the modified Cu substrate based electrode than for the as-received Cu substrate based electrode, which drops down to the cut-off voltage ( $0.005 \text{ V}$ ) at the  $\sim 600$ th cycle. When the end-of-discharge voltage reaches this value, the discharge capacity starts falling (Fig. 8a). This reflects in this latter case an increase with cycling of the lithium composition into less numerous electroactive Si particles in order to get the imposed  $1200 \text{ mAh g}^{-1}$  capacity [4]. For the modified Cu substrate based electrode, the fact that the end-of-discharge voltage at the 1000th cycle is much higher ( $0.09 \text{ V}$ ) than the cut-off voltage ( $0.005 \text{ V}$ ) suggests that such a process is minimized and it can be assumed that its cycling could be prolonged well beyond 1000 cycles.

On the other hand, the current collector roughening has a minor influence on the rate capability of the composite electrode as shown in Fig. 9, which compares the rate capability of the as-received and modified Cu substrate based electrodes. This may reflect the fact that their high-rate capability is mainly controlled by lithium mass transport constraints [4,28], which is not influenced by the current collector architecture.

#### 4. Conclusion

It was demonstrated that an appropriate electrochemical surface pre-treatment of the copper current collector, making a 3D network of Cu nanowires, remarkably improves the cycle life of a Si composite anode for Li-ion batteries. This roughened surface structure provides an enlarged interfacial contact area enhancing the adhesion of the Si-based coating on the current collector. As a result, a great decrease of the irreversible capacity associated with the electrical disconnection of the Si particles with cycling is observed, resulting in a significant improvement of the electrode

cycle life. Finally, it was shown that a micrometric Si-based electrode is able to maintain a discharge capacity of  $1200 \text{ mAh g}^{-1}$  for at least 1000 cycles by the conjunction of different strategies, namely: (i) the use of nanocrystalline (ball-milled) Si powder which induces a smoother phase transition upon cycling [29]; (ii) the use of CMC binder prepared in acid solution favouring the covalent grafting of the CMC binder to the Si particles [30]; (iii) the use of FEC + VC electrolyte additives resulting in less electrolyte decomposition at the surface of Si particles [5]; and (iv) the use of a properly roughened Cu current collector increasing the adhesion of the Si-based coating.

## Acknowledgements

Financial funding from the Agence Nationale de la Recherche (ANR) of France (BASIC project) and the Natural Science and Engineering Research Council (NSERC) of Canada is acknowledged.

## References

- [1] L.Y. Beaulieu, K.W. Eberman, R.L. Turner, L.J. Krause, J.R. Dahn, *Electrochem. Solid-State Lett.* 4 (2001) A137–A140.
- [2] J.H. Ryu, J.W. Kim, Y.-E. Sung, S.M. Oh, *Electrochem. Solid-State Lett.* 7 (2004) A306–A309.
- [3] M. Winter, *Zeit. Phys. Chem.* 223 (2009) 1395–1406.
- [4] Y. Oumellal, N. Delpuech, D. Mazouzi, N. Dupré, J. Gaubicher, P. Moreau, P. Soudan, B. Lestriez, D. Guyomard, *J. Mater. Chem.* 21 (2011) 6201–6208.
- [5] D. Mazouzi, N. Delpuech, Y. Oumellal, M. Gauthier, M. Cerbelaud, J. Gaubicher, N. Dupré, P. Moreau, D. Guyomard, L. Roué, B. Lestriez, *J. Power Sources* 220 (2012) 180–184.
- [6] U. Kasavajjula, C. Wang, A.J. Appleby, *J. Power Sources* 163 (2007) 1003–1039.
- [7] W.-J. Zhang, *J. Power Sources* 19 (2011) 13–24.
- [8] J.R. Szczech, S. Jing, *Energy Environ. Sci.* 4 (2011) 56–72.
- [9] Y.E. Roginskaya, T.L. Kulava, A.M. Skundin, M.A. Bruk, E.N. Zhikharev, V.A. Kal'nov, *Russ. J. Electrochem.* 44 (2008) 992–1001.
- [10] K.-L. Lee, J.-Y. Jung, S.-W. Lee, H.-S. Moon, J.-W. Park, *J. Power Sources* 129 (2004) 270–274.
- [11] H. Guo, H. Zhao, C. Yin, W. Qiu, *Mater. Sci. Eng. B* 131 (2006) 173–176.
- [12] J.-B. Kim, S.-H. Lim, S.-M. Lee, *J. Electrochem. Soc.* 153 (2006) A455–A458.
- [13] T. Takamura, S. Ohara, M. Uehara, J. Suzuki, K. Sekine, *J. Power Sources* 129 (2004) 96–100.
- [14] T. Takamura, M. Uehara, J. Suzuki, K. Sekine, K. Tamura, *J. Power Sources* 158 (2006) 1401–1404.
- [15] C.C. Nguyen, S.-W. Song, *Electrochim. Acta* 55 (2010) 3026–3033.
- [16] M. Uehara, J. Suzuki, K. Tamura, K. Sekine, T. Takamura, *J. Power Sources* 146 (2005) 441–444.
- [17] T. Zhang, H.P. Zhang, L.C. Yang, B. Wang, Y.P. Wu, T. Takamura, *Electrochim. Acta* 53 (2008) 5660–5664.
- [18] C.-M. Hwang, C.-H. Lim, J.-H. Yang, J.-W. Park, *J. Power Sources* 194 (2009) 1061–1067.
- [19] C.-M. Hwang, J.-W. Park, *Electrochim. Acta* 56 (2011) 6737–6747.
- [20] H. Li, F. Cheng, Z. Zhu, H. Bai, J. Tao, J. Chen, *J. Alloys Compd.* 509 (2011) 2919–2923.
- [21] W. Xu, N.L. Canfield, D. Wang, J. Xiao, Z. Nie, X.S. Li, W.D. Bennet, C.C. Bonham, J.-G. Zhang, *J. Electrochem. Soc.* 157 (2010) A765–A769.
- [22] H. Wolf, Z. Pajkic, T. Gerdes, M. Willert-Porada, *J. Power Sources* 190 (2009) 157–161.
- [23] X. Chen, K. Gerasopoulos, J. Guo, A. Brown, C. Wang, R. Ghodssi, J.N. Culver, *Adv. Funct. Mater.* 21 (2011) 380–387.
- [24] C. Yu, T. Ma, J. Rong, R. Zhang, J. Shaffer, Y. An, Q. Liu, B. Wei, H. Jiang, *Adv. Energy Mater.* 2 (2012) 68–73.
- [25] Y.-L. Kim, Y.-K. Sun, S.-M. Lee, *Electrochim. Acta* 53 (2008) 4500–4504.
- [26] T. Jiang, S. Zhang, X. Qiu, W. Zhu, L. Chen, *Electrochim. Commun.* 9 (2007) 930–934.
- [27] Q. Sa, Y. Wang, *J. Power Sources* 208 (2012) 46–51.
- [28] S. Rousselot, M. Gauthier, D. Mazouzi, B. Lestriez, D. Guyomard, L. Roué, *J. Power Sources* 202 (2012) 262–268.
- [29] M. Gauthier, D. Mazouzi, D. Reyter, B. Lestriez, P. Moreau, B. Lestriez, D. Guyomard, L. Roué, *Energy Environ. Sci.* 2013, in press.
- [30] D. Mazouzi, L. Roué, D. Guyomard, B. Lestriez, *Electrochim. Solid State Lett.* 12 (2009) A215–A218.
- [31] D. Reyter, M. Odziemkowski, D. Bélanger, L. Roué, *J. Electrochem. Soc.* 154 (2007) K36–K44.
- [32] M. Gauthier, J. Danet, B. Lestriez, L. Roué, D. Guyomard, P. Moreau, *J. Power Sources* 227 (2013) 237–242.
- [33] A. Etiemble, H. Idrissi, L. Roué, *EWGAE Proc. E30* (2012) 1–9.